Acta Crystallographica Section B
Structural Science
ISSN 0108-7681

Coupling of the lactone-ring conformation with crystal symmetry in 6-hydroxy-4,4,5,7,8-pentamethyl-3,4-dihydrocoumarin

Armand Budzianowski and Andrzej Katrusiak*

Faculty of Chemistry, Adam Mickiewicz University, 60-780 Poznań, Grunwaldzka 6, Poland

Correspondence e-mail: katran@amu.edu.pl

Received 2 June 2001
Accepted 22 October 2001

Conformational disorder and inversions of the lactone ring induce structural transformations in the crystals of 6-hydroxy-4,4,5,7,8-pentamethyl-3,4-dihydrocoumarin, $C_{14}H_{18}O_3$. The onset of ordering of the lactone ring at 300 K proceeds continuously, changes the space group from $P2_1/m$ to $P2_1/c$ and doubles the unit cell; the abrupt inversion of the lactone rings at 225 K changes the crystal translational symmetry in the (010) plane. The mechanism combining the molecular conformation and dynamics with the crystal structure, its symmetry, and phase transitions is presented.

1. Introduction

Symmetry is one of the main characteristics of crystals, often linked to their physical and chemical properties. However, the symmetry of crystals is almost totally unpredictable, particularly in those of organic molecular substances. In recent years there has been much effort into engineering crystal structures with specific properties, particularly in the fields of organic metals, organic magnets (Kahn, 2000) or optoelectronic devices (Sheats & Barbara, 1999). The common goal of these studies is to synthesize a compound with specific intermolecular interactions which assemble the molecules into a crystal with the required properties (*e.g.* see Braga *et al.*, 1999). The crystal symmetry is the key issue in this type of work. For example, polar, non-centrosymmetric space groups are prerequisites for second-harmonic generation, piezo- and pyro-electric effects, ferroelectricity *etc.* (Etter, 1990).

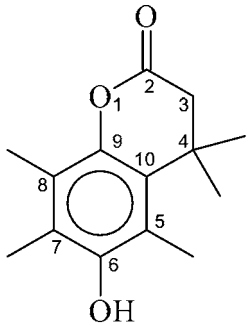

(1)

The symmetry of crystals is usually determined by the arrangement of molecules or ions and therefore the main concern in engineering crystals is the topology of functional groups in the molecules and their interactions, mainly hydrogen bonds (Ziener *et al.*, 2000) or coordination bonds, that assemble the molecules into a required supramolecular

structure. The molecular shape and the principle of close packing are of vital importance in these considerations (Kitajgorodski, 1976). However, the literature rarely contains studies of how intramolecular features, such as the conformations of molecules, determine the symmetry, transformations and properties of crystals (Katrusiak, 1991, 2000; Bernstein & Hagler, 1978). In this report we present our investigation into the structures and symmetry transformations of 6-hydroxy-4,4,5,7,8-pentamethyl-3,4-dihydrocoumarin [denoted (1), see (I) and Fig. 1], which are induced mainly by intramolecular inversions, both static and dynamic, of the lactone ring. Our interest in (1) originates from the previous study on stereopopulation effects of the trimethyl lock (Milstien & Cohen, 1972; Brochardt & Cohen, 1972*a*,*b*; Karle & Karle, 1972). It has been shown that the trimethyl lock of methyls C41, C42 and C51 has no significant effect on molecular conformation (Katrusiak, 1996*a*).

Crystal (1) undergoes two phase transitions which differ in their thermodynamic character, but in both cases the structural transformations are almost entirely confined to the molecular conformation. We have characterized the stability of the crystal by difference thermal analysis (DTA), measured the unit-cell dimensions at ~60 temperatures and determined the crystal structure at 13 temperatures in order to map the structural changes and to understand the mechanisms of the phase transitions. The phase transitions of (1) exemplify the correlation between soft conformational parameters and the symmetry of crystal lattices, as well as the possibility of employing the intramolecular transformations for designing transformable crystal structures.

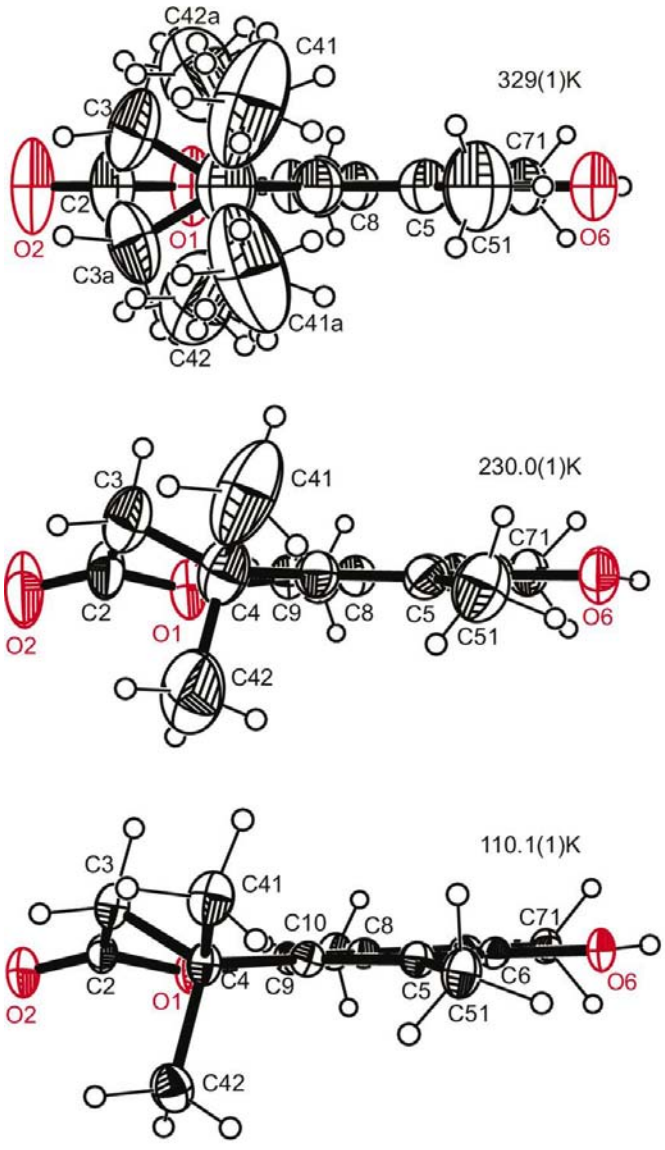

Figure 1
ORTEP (Johnson, 1965) views along the phenyl ring of molecule (1) in phase I at 329 K, in phase II at 230 K and in phase III at 110 K. Both sites for each disordered atom are shown for the molecule at 329 K, while only the main sites have been included for the molecule at 230 K. Displacement ellipsoids have been drawn at 50% probability level and the H atoms are indicated as small circles.

2. Experimental

2.1. X-ray determination

The crystal structures of (1) were investigated by X-ray single-crystal diffraction at 110, 150, 220, 222, 224, 225, 226, 228, 230, 250, 278, 285 and 293 K, using a Kuma KM-4 four-circle CCD diffractometer equipped with a graphite monochromator (Mo $K\alpha$ radiation, λ = 0.71073 Å) and Oxford Cryosystems cooler device CPC611. The crystal-to-detector distance was 80 mm. The structure determinations at 306, 317 and 328 K, and unit-cell determinations at 44 temperatures between 110 and 328 K, were carried out using a Kuma KM-4 diffractometer with a single-point detector and a graphite monochromator. This diffractometer was equipped with attachments: an Oxford Instruments cooler device (ILM201, Cryojet Controller) and a high-temperature air-stream heater constructed in our laboratory. The structures were solved by direct methods (Sheldrick, 1986) and refined with anisotropic thermal parameters by full-matrix least-squares (Sheldrick, 1997). All H atoms were located from difference-Fourier maps and refined with isotropic thermal parameters, except for the H atoms at disordered atoms C3, C41 and C42 in the structures of phase II at temperatures of 225 and 285 K, where the H atoms were placed in geometrically idealized positions after each cycle of refinement. The details of the exemplary determinations at 150 K (phase III), 225 and 285 K (phase II) and 306 K (phase I) are listed in Table 1; the atomic coordinates for the structures at these temperatures and the full documentation for all structural determinations at 13 temperatures have been deposited as supplementary data.[1] The DTA signal was measured for a polycrystalline sample in the temperature

[1] Supplementary data for this paper with the complete structural data measured at 110, 150, 220, 222, 224, 225, 226, 228, 230, 250, 278, 285, 293, 306, 317 and 328 K are available from the IUCr electronic archives (Reference: BM0046). Services for accessing these data are described at the back of the journal.

Table 1
Crystal data and refinements for 6-hydroxy-4,4,5,7,8-pentamethyl-3,4-dihydrocoumarin at 150 K (phase III), 225 and 285 K (phase II) and at 306 K (phase I).

These are exemplary structures of a series of varied temperature determinations – see footnote **1**.

	Phase III	Phase II	Phase II	Phase I
Temperature (K)	150.0 (1)	225.1 (1)	285.0 (1)	306 (2)
Empirical formula	C_{14} H_{18} O_3			
Formula weight	234.28			
Wavelength (Å)	0.71073	0.71073	0.71073	1.54178
Crystal system	Monoclinic			
Space group	$P2_1/n$	$P2_1/c$	$P2_1/c$	$P2_1/m$
Unit-cell dimensions				
a (Å)	13.429 (4)	9.760 (7)	9.768 (6)	9.753 (2)
b (Å)	6.784 (2)	6.863 (2)	6.933 (3)	6.9330 (10)
c (Å)	13.792 (4)	19.113 (4)	19.130 (4)	9.572 (2)
β (°)	91.54 (2)	94.75 (4)	94.39 (4)	94.39 (3)
Volume (Å ^{3})	1256.0 (6)	1275.8 (10)	1291.7 (10)	645.3 (2)
Z	4	4	4	2
Density (calculated) (g cm^{-3})	1.239	1.220	1.205	1.206
Absorption coefficient (mm^{-1})	0.086	0.085	0.084	0.676
F(000) (e)	504	504	504	252
Crystal size (mm)	0.35 × 0.25 × 0.12	0.30 × 0.25 × 0.12	0.44 × 0.38 × 0.12	0.35 × 0.25 × 0.12
Min/max θ for data (°)	3.03/30.15	3.63/29.53	3.72/29.57	4.55/60.10
Ranges of indices				
h	−18 → 18	−13 → 13	−6 → 13	−10 → 10
k	−9 → 5	−9 → 5	−9 → 9	0 → 7
l	−18 → 1	−26 → 25	−26 → 25	0 → 10
Reflections collected	10 354	7747	7944	1106
Unique reflections (R_{int})	3323 (0.0303)	3276 (0.0520)	3313 (0.0199)	1045 (0.0263)
Refinement method	Full-matrix least-squares on F^2			
Data/parameters	3323/227	3276/216	3313/275	1045/157
Goodness-of-fit on F^2	0.999	0.985	1.038	0.930
Final R_1/wR_2 ($I > 2\sigma_I$)	0.0549/0.1261	0.0558/0.0716	0.0642/0.1951	0.0468/0.1029
R_1/wR_2 indices (all data)	0.1049/0.1522	0.2229/0.0850	0.1131/0.2248	0.0556/0.1094
Extinction coefficient	0.0007 (13)	0.016 (5)	0.002 (3)	0.048 (2)
Max. difference peak/hole (e Å^{-3})	0.337/−0.218	0.247/−0.178	0.348/−0.220	0.161/−0.135

range 100–340 K, with the temperature ramp rate of ±5 K min^{-1}.

3. Results and discussion

3.1. Second-order phase transition at T_{12} = 300 K

Bond lengths and valence angles (Table 2) confirm the molecular structure shown in (I). Molecule (1) (see Fig. 1) is planar, except for atom C3 of the lactone ring and the two methyl groups at C4. Small distortions from planarity for the phenyl ring (see Table 3), consistently observed in the structures determined at low temperatures, are caused by steric effects due to overmethylation (Karle & Karle, 1972; Katrusiak, 1989*a*,*b*). The lactone ring assumes the sofa conformation, but two equivalent sites of C3 relative to the molecular plane can be distinguished. The positions of two adjacent methyl groups C41 and C42 on C4 are coupled to the position of C3. Thus, the potential energy of the ring can be described by a double-well function with a barrier separating two minima of C3, corresponding to two sofa conformations with C3 displaced to the opposite sides of the molecular plane: these two sites for C3 are denoted C3 and C3′. If the molecules were raised in energy above the barrier, the lactone rings would become dynamically disordered. Indeed, we have observed this disorder by X-ray diffraction in crystals of (1) above 300 K. On lowering the temperature below 300 K, C3 and adjacent methyl groups gradually start to order, breaking the mirror symmetry of the molecules, and the crystal undergoes a second-order phase transition at T_{12} = 300 K.

The process of freezing the lactone ring inversion proceeds well below 300 K and comes to a complete halt only at 225 K. The continuous character of the phase transition is also confirmed by the DTA study (see Fig. 2) and by the continuous change of the unit-cell dimensions (see Fig. 3). These measurements also indicated another phase transformation for crystals (1), at T_{23} = 225 K. The DTA signal and the thermal expansion anomalies show that the phase transition at 225 K is first-order. In the following discussion the high-temperature phase of (1) is labelled as I, the intermediate phase as II and the low-temperature phase as III.

The crystal structures shown in Fig. 4 clearly demonstrate that the molecular arrangements in phases I, II and III are very similar. This is reflected in the straightforward relationship between the unit-cell parameters (the subscripts indicate the phases): the c_I translation of phase I doubles in phase II (*i.e.* $c_{II} = 2c_I$), while a_{III} and c_{III} of phase III lie along directions $[201]_{II}$ and $[\bar{2}01]_{II}$ of phase II, or along diagonals between a_I and c_I when referred to phase I (see Fig. 5). Thus, angle β in phase III is contained between diagonal directions $[101]_I$ and

Table 2
Bond lengths (Å) and angles (°) for 6-hydroxy-4,4,5,7,8-pentamethyl-3,4-dihydrocoumarin.

Temperature (K)	150.0 (1)	225.1 (1)	285.0 (1)	306 (2)
O1—C2	1.348 (2)	1.341 (2)	1.331 (2)	1.311 (4)
O2—C2	1.208 (2)	1.206 (3)	1.197 (3)	1.180 (4)
C2—C3	1.483 (3)	1.480 (3)	1.496 (4)	1.520 (6)
C3—C4	1.541 (3)	1.546 (3)	1.542 (3)	1.561 (6)
C4—C41	1.533 (3)	1.546 (4)	1.549 (4)	1.587 (10)
C4—C42	1.535 (3)	1.544 (4)	1.528 (4)	1.480 (10)
C4—C10	1.540 (2)	1.521 (3)	1.537 (2)	1.536 (4)
C5—C10	1.405 (2)	1.396 (3)	1.404 (2)	1.403 (4)
C5—C51	1.511 (2)	1.509 (3)	1.514 (3)	1.512 (5)
C5—C6	1.405 (2)	1.396 (3)	1.399 (2)	1.391 (4)
C6—O6	1.373 (2)	1.380 (2)	1.371 (2)	1.378 (3)
C6—C7	1.400 (2)	1.393 (2)	1.401 (3)	1.388 (4)
C7—C71	1.508 (2)	1.502 (3)	1.508 (2)	1.505 (4)
C7—C8	1.396 (2)	1.397 (3)	1.388 (2)	1.392 (4)
C8—C81	1.504 (2)	1.515 (3)	1.509 (3)	1.502 (4)
C8—C9	1.396 (2)	1.390 (2)	1.400 (2)	1.390 (4)
C9—C10	1.398 (2)	1.387 (2)	1.395 (2)	1.379 (4)
O1—C9	1.4131 (19)	1.429 (2)	1.403 (2)	1.409 (3)
C10—C4—C3	107.17 (14)	108.45 (19)	107.47 (16)	106.4 (3)
C10—C4—C41	115.13 (16)	113.8 (2)	112.9 (2)	112.0 (4)
C10—C4—C42	109.25 (15)	109.8 (2)	109.64 (19)	110.4 (4)
C10—C5—C51	124.10 (16)	124.0 (2)	125.00 (17)	124.7 (3)
C10—C9—O1	121.57 (14)	121.86 (19)	122.53 (15)	122.2 (2)
C2—C3—C4	112.67 (16)	113.0 (2)	112.49 (19)	109.5 (4)
C2—O1—C9	121.37 (13)	121.21 (18)	122.16 (16)	123.4 (3)
C3—C4—C41	104.86 (16)	104.5 (2)	103.9 (2)	101.8 (4)
C41—C4—C42	110.27 (18)	110.9 (3)	113.0 (3)	113.7 (7)
C42—C4—C3	109.97 (16)	109.2 (2)	109.6 (3)	112.0 (5)
C5—C10—C4	126.06 (15)	126.3 (2)	125.40 (17)	125.7 (3)
C6—C5—C10	119.01 (15)	119.2 (2)	118.70 (16)	118.7 (3)
C6—C5—C51	116.84 (15)	116.7 (2)	116.26 (17)	116.7 (3)
C6—C7—C71	119.24 (15)	120.1 (2)	119.64 (15)	120.3 (3)
C7—C6—C5	122.73 (14)	123.2 (2)	122.76 (15)	123.5 (2)
C7—C8—C81	122.08 (15)	121.7 (2)	122.49 (16)	121.8 (3)
C7—C8—C9	117.94 (15)	117.2 (2)	118.10 (15)	117.6 (3)
C8—C7—C6	118.70 (15)	118.2 (2)	118.84 (15)	118.2 (3)
C8—C7—C71	122.02 (16)	121.7 (2)	121.51 (17)	121.5 (3)
C8—C9—C10	124.53 (14)	125.69 (19)	123.89 (15)	125.2 (2)
C8—C9—O1	113.67 (14)	112.19 (18)	113.45 (15)	112.6 (2)
C9—C10—C4	116.91 (14)	117.41 (19)	116.96 (16)	117.5 (3)
C9—C10—C5	116.99 (15)	116.3 (2)	117.63 (16)	116.8 (3)
C9—C8—C81	119.98 (15)	121.0 (2)	119.41 (16)	120.6 (3)
O1—C2—C3	115.56 (15)	115.5 (2)	114.44 (17)	110.2 (3)
O2—C2—C3	127.07 (16)	126.6 (2)	126.5 (2)	121.5 (3)
O2—C2—O1	117.36 (17)	117.7 (2)	118.3 (2)	120.5 (4)
O6—C6—C5	116.02 (15)	115.8 (2)	115.66 (17)	115.3 (3)
O6—C6—C7	121.25 (15)	120.9 (2)	121.57 (16)	121.2 (3)

Table 3
Selected torsion angles (°) for 6-hydroxy-4,4,5,7,8-pentamethyl-3,4-dihydrocoumarin.

Temperature (K)	150.0 (1)	225.1 (1)	285.0 (1)	306 (2)
Lactone ring				
O1—C2—C3—C4	−44.1 (2)	−44.2 (4)	−48.4 (3)	−60.0 (4)
C2—C3—C4—C10	54.9 (2)	51.9 (4)	53.7 (2)	57.7 (4)
C3—C4—C10—C9	−30.0 (2)	−25.9 (4)	−27.2 (2)	−28.8 (3)
O1—C9—C10—C4	−6.9 (2)	−9.0 (4)	−6.4 (2)	0
C9—O1—C2—C3	4.6 (2)	7.3 (4)	12.8 (3)	30.4 (3)
C10—C9—O1—C2	22.4 (2)	20.7 (4)	15.8 (2)	0
Phenyl ring				
C5—C6—C7—C8	−0.5 (2)	−1.7 (4)	−1.3 (2)	0
C6—C7—C8—C9	1.1 (2)	2.4 (4)	1.51 (19)	0
C7—C8—C9—C10	0.7 (3)	−0.1 (4)	0.6 (2)	0
C8—C9—C10—C5	−3.1 (3)	−3.0 (4)	−2.9 (2)	0
C9—C10—C5—C6	3.6 (2)	3.7 (4)	3.01 (19)	0
C10—C5—C6—C7	−2.0 (3)	−1.5 (4)	−1.0 (2)	0
Exocyclic angles				
O2—C2—C3—C4	136.8 (2)	139.2 (4)	141.5 (2)	150.8 (3)
C9—O1—C2—O2	−176.27 (16)	−175.8 (3)	−176.27 (16)	180
C9—C10—C4—C41	−146.16 (18)	−141.5 (3)	−141.2 (3)	−139.3 (4)
C9—C10—C4—C42	89.2 (2)	92.8 (3)	91.9 (3)	92.9 (6)
C5—C10—C4—C3	152.33 (18)	154.9 (3)	153.96 (18)	151.2 (3)
C5—C10—C4—C41	36.1 (3)	39.3 (4)	39.9 (3)	40.7 (4)
C5—C10—C4—C42	−88.6 (2)	−86.4 (4)	−87.0 (3)	−87.1 (6)
O6—C6—C7—C8	179.31 (16)	178.0 (2)	178.70 (13)	180
O6—C6—C5—C10	178.22 (16)	178.7 (2)	178.96 (12)	180
O6—C6—C7—C71	1.4 (2)	0.6 (4)	0.3 (2)	0
O6—C6—C5—C51	−4.5 (2)	−4.8 (4)	−3.4 (2)	0

$[10\bar{1}]_{\rm I}$ in phase I and the monoclinic angle shown in Fig. 5 is the β angle of the unit cells in phases I and II, and its equivalent in phase III (*i.e.* the angle between $[10\bar{1}]_{\rm III}$ and $[101]_{\rm III}$).

The gradual process of the lactone ring ordering below T_{12} is strongly non-linear with temperature. This can be observed both from the continuous changes in the intensities of these reflections which become extinct above T_{12}, as exemplified by the intensity of reflection (213) shown in Fig. 6, and by the occupation factors of the C3 and C3′ sites shown in Fig. 7, obtained from the structure refinements. In these refinements the occupancies of the methyl atoms C41 and C42, as well as C41′ and C42′, which are coupled with the positions of the disordered atom C3, were constrained to the respective occupancies of C3 and C3′. It can be seen that the 50:50 occupation above T_{12} changes to 79.5:20.5 at $T = (T_{12} - 7)$ K, to 90.4:9.6 at $(T_{12} - 22)$ K and to 96.5:3.5 at $(T_{12} - 40)$ K. At temperatures close to T_{23} small difference electron-density features at C3′, C41′ and C42′ testify to some remaining disorder in the lactone ring, although the ratio of the occupancies of C3:C3′ is estimated as ∼98.9:1.1 from the measurement at $(T_{12} - 70)$ K [*i.e.* $(T_{23} + 5)$ K]. The crystal symmetry change is directly connected to the freezing of the lactone ring inversions (as described above): the molecules are translationally identical along $[001]_{\rm I}$ when C3 is 50:50 disordered above T_{12} (see Fig. 7), but below T_{12} the C3 atoms of

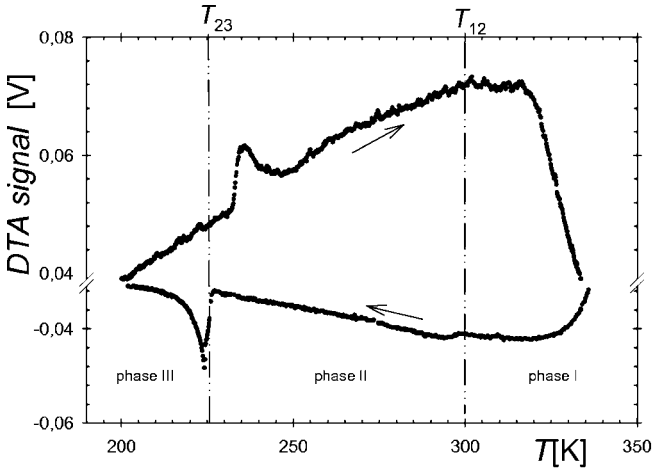

Figure 2
DTA signal of the 6-hydroxy-4,4,5,7,8-pentamethyl-3,4-dihydrocoumarin crystal. The heating and cooling runs are indicated by arrows.

neighbouring molecules start to order on the opposite sides of the rings. Thus, below T_{12} the neighbouring molecules are no longer related by a translation along $[001]_{I}$, only every second molecule has the lactone ring inverted in the same direction and we observe doubling of the length of the c axis below T_{12}.

The dynamical lactone ring inversions in temperatures above T_{23} = 225 K are also corroborated by large vibrational parameters of atoms C3, C41 and C42 perpendicular to their molecular plane (see Fig. 1).

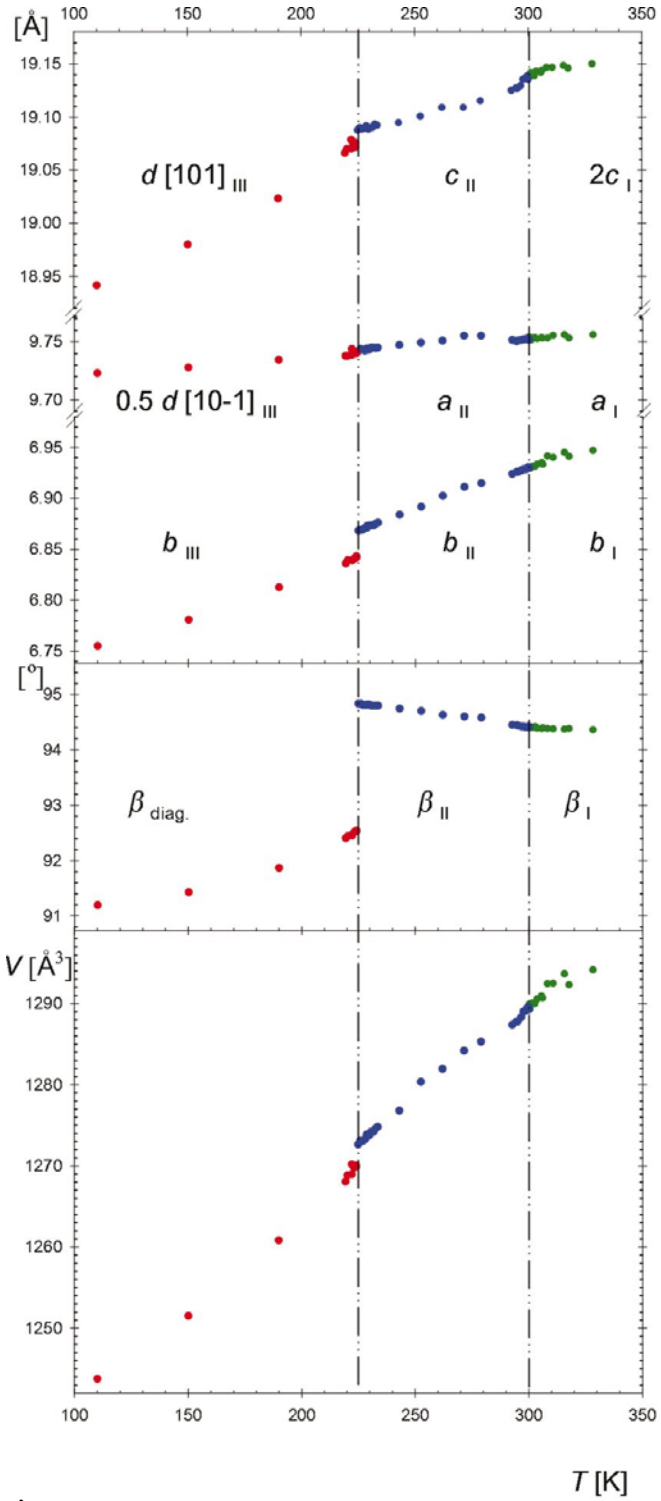

Figure 3
Unit-cell dimensions of (1) as a function of temperature. Unit-cell parameters a, b, c, β and V have been transformed to the unit cell of phase II for convenient comparison. Thus, for example, the angle between diagonal directions [101] and [10$\bar{1}$] in phase III corresponds to the β angles in phases I and II.

3.2. First-order phase transition at T_{23} = 225 K

When the dynamical disorder of C3, C41 and C42 is frozen out at T_{23} = 225 K, abrupt inversions of the lactone ring occur in every second molecule along $[100]_{II}$, as shown schematically in Fig. 8. This transformation is clearly first-order (see Figs. 2 and 3) and it changes the direction of the principal crystal translation **a**. Translations **b** and **c** remain the same as in phase II, but the **c** vector has been redefined to avoid a very acute angle β, as shown in Figs. 5 and 8. The matrix transforming the unit cell from phase II to phase III is

$$M_{23} = \begin{pmatrix} 1 & 0 & 0.5 \\ 0 & 1 & 0 \\ -1 & 0 & 0.5 \end{pmatrix}.$$

In addition to the change in the principal translation along $[100]_{II}$, there is also an intriguing change to the space-group symmetry. The space group $P2_1/c$ remains unchanged for the unit cells with the c axis common for phases II and III, which is equivalent to space group $P2_1/n$ for the choice of axes implemented in phase III (as explained above), but the sites of the centres of symmetry and of the screw axes at x_{II} = 0.5 are interchanged (or shifted to z_{II} + 0.25). This interchange of the $\bar{1}$ and 2_1 sites is possible in the crystals of (1) due to their pseudosymmetry: the lactone ring is the main structural factor determining which of these symmetry elements relates the neighbouring molecules. If the C3 atoms of two neighbouring molecules are displaced from their molecular planes in the same direction, then the molecules are related by the 2_1 screw axis; if the lactone rings are inverted in opposite directions then the molecules are related by the inversion centre. Thus, in other words, the phase transition at T_{23} involves the inversion of the lactone ring in every second molecule in hydrogen-bonded chains along $\mathbf{a}_{II}$. In temperatures above T_{12}, in phase I the lactone rings are dynamically disordered with equal occupancies, the two symmetries superimpose and the crystal acquires a mirror symmetry along the molecular plane.

Distortions of the crystal structure from 'prototypical' high-temperature phase I still increase in phase III and are reflected in the increased intensities of reflections which become extinct above T_{12}, as shown in Fig. 9. The structural origins of the these distortions are not limited to the intramolecular factors of the lactone ring conformation, as in phase II, but a significant contribution arises from the arrangement of the molecules in the crystal lattice. It can be seen in Fig. 10 that the molecules are parallel to (010) in phase I and in phase II they are tilted to this plane only by ~0.5°. However, at T_{23} the tilt increases to ~2° and at 150 K it is already saturated at over 3°. It is apparent that the dynamical inversions of the lactone ring stabilize the parallel positions of the molecules. It can also be

shown that the tilts are significant factors in the mechanism of the phase transition at T_{23}. As can be seen from the projections along $[100]_{II}$ presented in Fig. 4, the overlapping molecules have atoms C3 of the lactone rings in the sofa conformations directed in the same sense along [010] – upwards for the pair of molecules closest to the origin in this drawing. These two molecules are related by the 2_1 screw axis, as explained above. The bulk of the molecule is displaced along [010] in the opposite sense relative to C3 and the displacement of the terminal atoms about hydroxyl O6H depends on the sense of the inversion of C3. In phase II the angle between the planes of the partly overlapping molecules is equal to the double tilt angle ρ (Fig. 10) and it increases as the temperature is lowered from T_{12} to T_{23}. However, at T_{23} the two partly overlapping molecules become related by a centre of symmetry, which requires that their molecular planes be parallel. This is the main structural factor explaining the occurrence of the phase transition and the symmetry change at T_{23}. Large-amplitude vibrations of C3, C41 and C42 and inversions of the lactone ring stabilize the parallel arrangement of the molecules in phase I, and even their small tilts in phase II do not significantly increase the interaction between the overlapping molecules. However, when the lactone-ring inversions freeze in low temperatures, the space required for the large amplitude vibrations of C3, C41 and C42 become vacant at the lactone end of the molecule (see Fig. 4). This empty space is filled at T_{23}, when the lactone rings in every second sheet along [010] are inverted and when, due to the symmetry changes, the molecular planes of the overlapping molecules become parallel. Thus, the strongest parameter contraction is along [010] and the most marked volume change occurs at T_{23}.

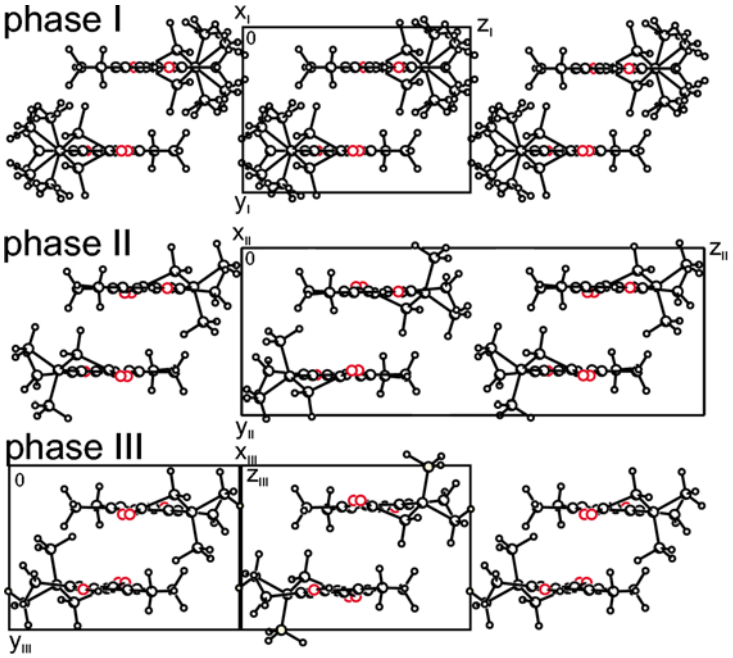

Figure 4
Views of the molecular arrangements projected onto (010) in phases I, II and III. Both sites of the disordered atoms are shown for phase I, but for clarity only the higher occupancy sites for C3, C41 and C42 are shown for phase II.

Table 4
Hydrogen-bonding parameters in selected temperatures of phases III, II and I of 6-hydroxy-4,4,5,7,8-pentamethyl-3,4-dihydrocoumarin.

Temperature (K)	150.0 (1)	220.0 (1)	225.1 (1)	285.0 (1)	306 (2)
O6···O2^{i}	2.819 (2)	2.833 (2)	2.820 (4)	2.818 (3)	2.820 (4)
O6—H6	0.85 (3)	0.85 (3)	0.87 (4)	0.96 (3)	0.88 (5)
H6---O2^{i}	2.02 (3)	2.02 (3)	1.99 (4)	1.90 (3)	2.00 (5)
O6—H6---O2^{i}	157 (2)	161 (2)	160 (3)	160 (3)	154 (4)
C6—O6···O2^{i}	128.6 (1)	129.1 (1)	129.1 (2)	129.4 (1)	129.3 (2)
O6···O2^{i}—C2^{i}	121.5 (1)	121.6 (1)	122.9 (2)	123.4 (2)	124.3 (3)
C6—O6···O2^{i}—C2^{i}	−166 (2)	−166 (2)	166 (3)	169 (2)	180

Symmetry codes: (i) $\frac{1}{2}+x, \frac{1}{2}+y, z-\frac{1}{2}$ in phase III (150, 220 K); (i) $1+x, y, z$ in phase II (225, 285 K) and in phase I (306 K).

3.3. Temperature dependence of the OH---O bond

The relatively weak —O6—H6- - -O2′═C2′ hydrogen bond (see Table 4) is the strongest of intermolecular interactions in structure (1) and the phase transitions can be considered in terms of transformations of the hydrogen-bonded supramolecular aggregate (Katrusiak, 1998). It can be seen from Figs. 11 and 12 that the O···O distance and Donohue angles (Katrusiak, 1996*b*) are only slightly affected at the phase transitions. This indicates that no strains in the hydrogen bond are induced or released at the phase transitions and that, compared with the other crystal cohesion forces, the role of the hydrogen bond does not significantly change at the phase transitions. The most marked change in the geometry of the hydrogen bond occurs at T_{12} for its torsion C6—O6···O2′—C2′, denoted $\tau_{O\cdots O}$ in Fig. 12. The value of $\tau_{O\cdots O}$ depends both on the mutual orientation of the hydrogen-bonded molecules, to some extent expressed by the inclinations of the molecules to crystal planes (010) shown in Fig. 10, and on the conformation of the lactone ring, all atoms of which except C3 are confined to the mirror plane in phase I. The displacement of O2 off the molecular plane can be measured by the torsion angle O2—C2—O1—C9 plotted in Fig. 12. As can be seen from Fig. 12 and the torsion angles from Table 4, the endocyclic torsion angle O2—C—O1—C9 changes significantly at T_{12}, but only slightly and in the opposite direction at T_{23}. The hydrogen-bond torsion $\tau_{O\cdots O}$ exhibits similar temperature dependence: it changes abruptly at the continuous phase transition at T_{12} and the magnitude of this change reverses slightly at the first-order phase transition at T_{12} (Fig. 12). The tempera-

ture dependence of the molecular inclination ρ is different at the two phase transitions: at T_{12} the change of ρ is small, while at T_{23} it is much larger (see Fig. 10).

Changes in both the inclination of molecules and the O2—C2—O1—C9 torsion angles are consequences of sheer at the structural transformations at T_{12} and T_{23}. This would support the conclusion that the hydrogen bond does not contribute directly to the mechanism of the phase transitions, which are induced mainly by the conformational dynamics at T_{12} and van der Waals interactions between overlapping molecules at T_{23}.

However, it is remarkable that the temperature dependence of the hydrogen-bond dimensions is consistent with the general rules governing the changes of hydrogen-bond geometry depending on the thermodynamic character of the phase transitions (Katrusiak, 1993, 1995, 2001). These characteristic features are a shortening of the O···O distance on cooling through the continuous phase transition at T_{12} and a lengthening of O···O at the discontinuous phase transition at T_{23} (Fig. 11).

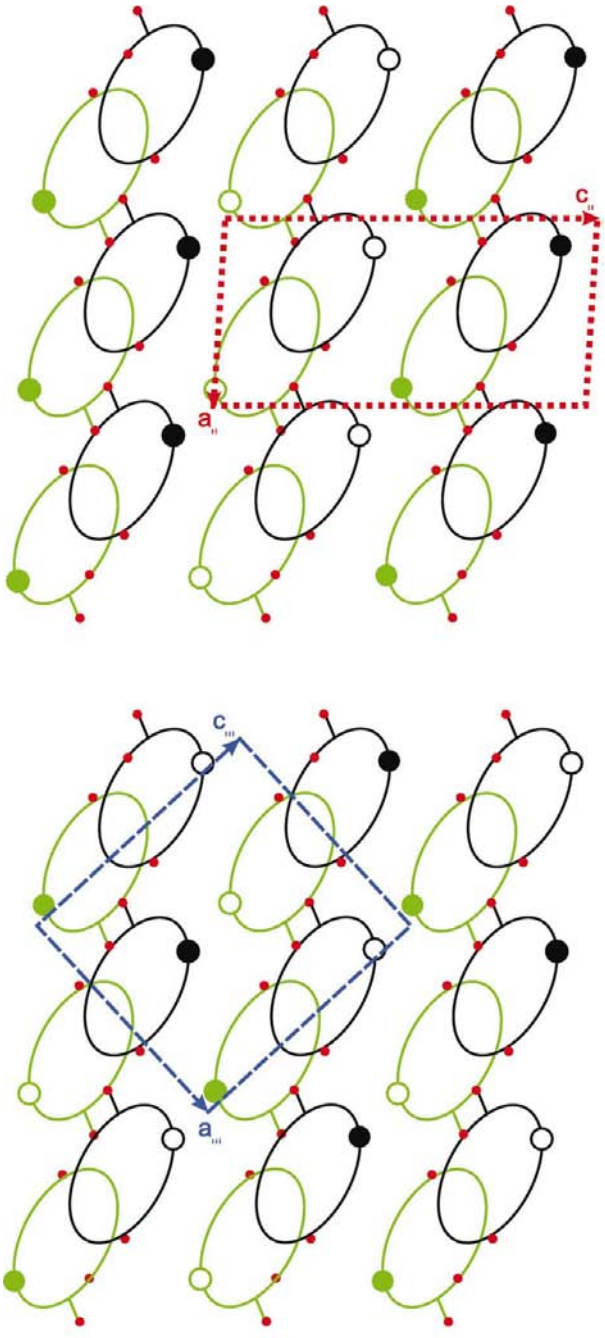

Figure 5
Projection of structure (1) down [010] with indicated unit-cell edges of phases I (thin green line), II (short red dashes) and III (long blue dashes); as well as the corresponding reciprocal spaces nodes: filled circles for phase I, both full and open circles for phase II, and both full circles and asterisks for phase III.

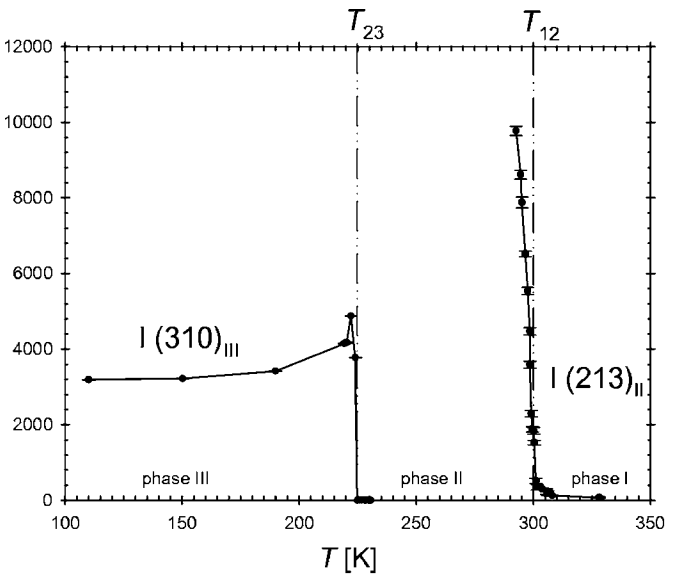

Figure 6
Intensities of reflections $(213)_{II}$ and $(310)_{III}$ as a function of temperature.

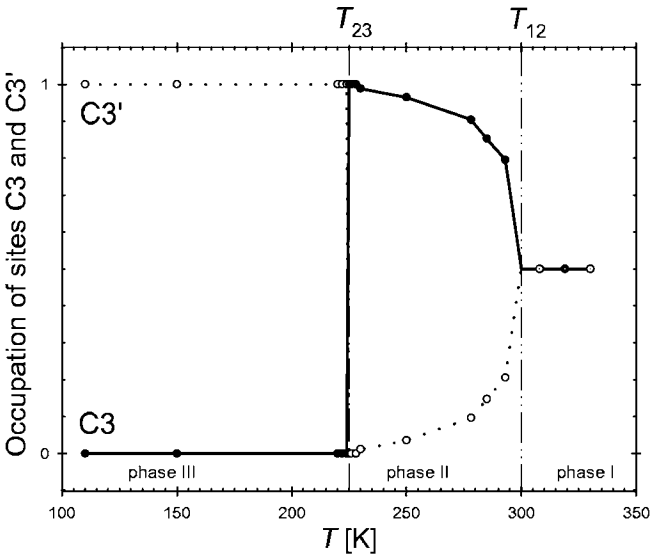

Figure 7
Temperature dependence of the occupancies of C3 (solid line) and C3′ (dotted line).

4. Conclusions

The phase transitions in crystal (1) are driven by the dynamic disorder and inversions of the molecular lactone ring. The lactone ring disorder at temperatures above $T_{12} = 300$ K is due to dynamic inversion between two equivalent sofa conformations. Ring-ordering proceeds continuously – begins below T_{12} and continues until $T_{23} = 225$ K when the molecules become fully ordered. The inversions of the lactone ring at T_{23} allow the molecules to pack more densely, hence the volume change and first-order phase transition. The behaviour of the lactone rings is directly connected to the crystal symmetry.

The main structural transformations at the phase transitions at T_{12} and T_{23} are due to changes in molecular conformation coupled to lattice dynamics of the crystal. Similar effects can occur in much more complex systems and may contribute to the properties and functions of macromolecules.

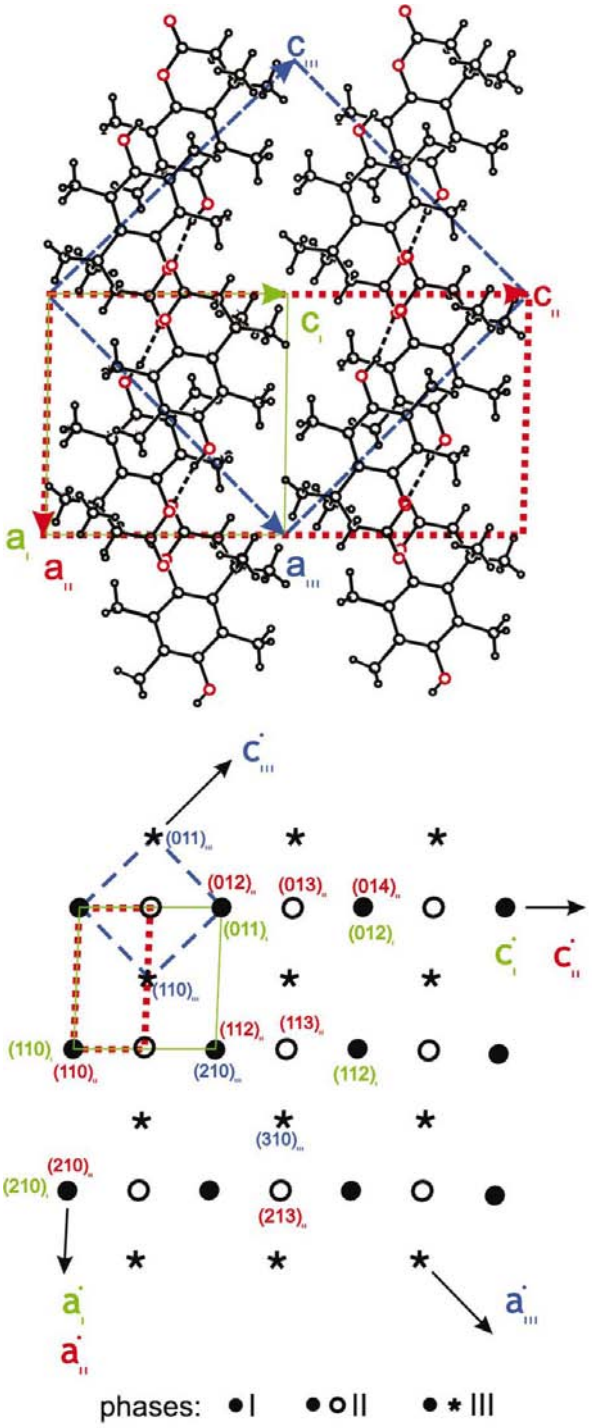

Figure 8
Schematic drawing of two sheets of molecules viewed down [101] in phases II and III (*cf.* Figs. 4 and 5). The molecules are represented as ovals; the large circles show methylene C3 directed upward (shaded) or downward (open); small red dots indicate the lactone O atoms and site of the hydroxyl groups. The molecules in the lower sheet are shown in green.

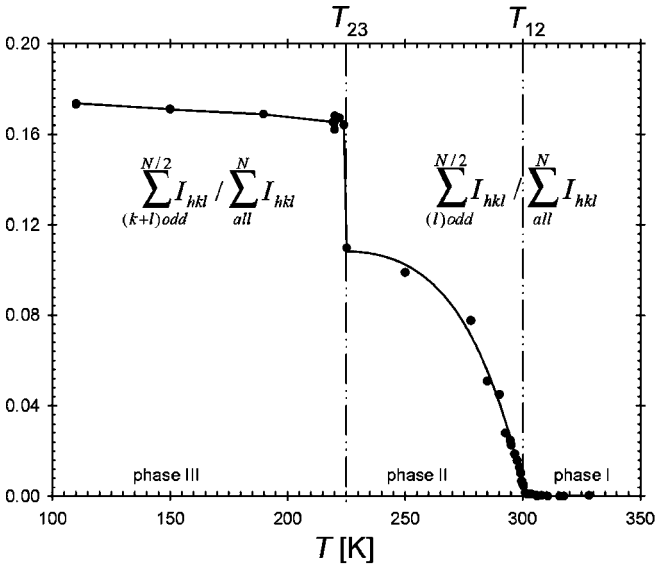

Figure 9
Temperature dependence of the ratio of the sum of intensities of reflections extinguished in phase I (see open circles and asterisks for phases II and III, respectively, in Fig. 5) to the sum of intensities of all reflections. The e.s.d.'s are smaller than the plotted symbols.

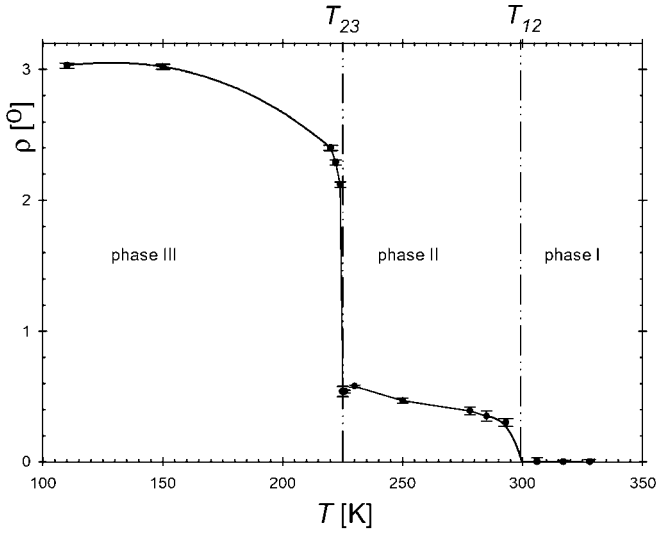

Figure 10
The temperature dependence of the inclination of the least-squares mean planes fitted to six C5–10 atoms to the crystal plane (010).

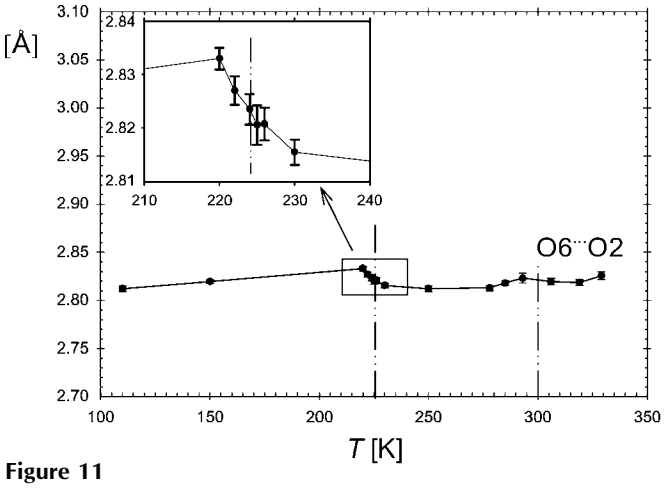

Figure 11
The temperature dependence of the O6···O2′ distance in the hydrogen bond (symmetry code: $\frac{1}{2}+x, \frac{1}{2}+y, z-\frac{1}{2}$ in phase III, and $1+x, y, z$ in phases I and II).

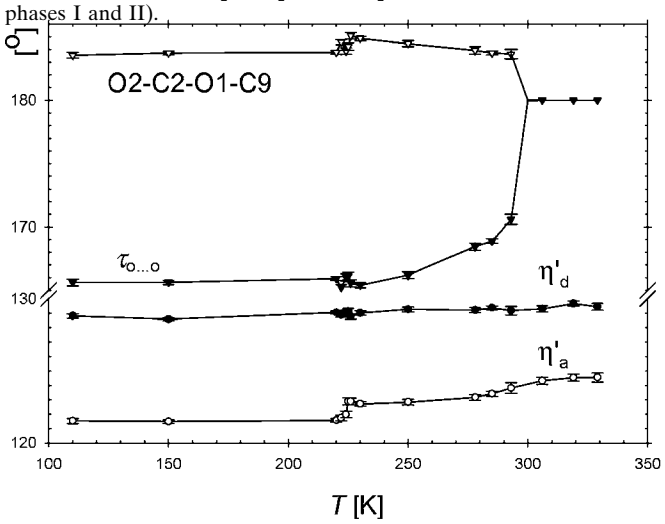

Figure 12
Donohue angles O6···O2′—C2′ (denoted η'_a), C6—O6···O2′ (η'_d), hydrogen-bond torsion angle C6—O6···O2′—C2′ (τ_{O-O}), and the endocyclic torsion O2—C2—O1—C9 in molecule 1 as a function of temperature.

We are grateful to Professor Wiesław Antkowiak of the Faculty of Chemistry, Adam Mickiewicz University, for providing the compound, and to Dr Marek Szafrański of the Faculty of Physics, Adam Mickiewicz University, for performing the DTA measurements.

References

Bernstein, J. & Hagler, A. T. (1978). *J. Am. Chem. Soc.* **100**, 673–681.
Braga, D., Grepioni, F. & Orpen, A. G. (1999). *Crystal Enginering: From Molecules and Crystals to Materials.* Dordrecht: Kluwer Academic Publishers.
Brochardt, R. T. & Cohen, L. A. (1972*a*). *J. Am. Chem. Soc.* **94**, 9166–9174.
Brochardt, R. T. & Cohen, L. A. (1972*b*). *J. Am. Chem. Soc.* **94**, 9175–9181.
Etter, M. C. (1990). *Acc. Chem. Res.* **23**, 120–126.
Johnson, C. K. (1965). *ORTEP.* Report ORNL-3194. Oak Ridge National Laboratory, Tennessee.
Kahn, O. (2000). *Acc. Chem. Res.* **33**, 647–657.
Karle, J. M. & Karle, I. M. (1972). *J. Am. Chem. Soc.* **94**, 9182–9189.
Katrusiak, A. (1989*a*). *Acta Cryst.* C**45**, 275–278.
Katrusiak, A. (1989*b*). *Acta Cryst.* C**45**, 1201–1205.
Katrusiak, A. (1991). *Acta Cryst.* B**47**, 398–404.
Katrusiak, A. (1993). *Phys. Rev. B*, **48**, 2992–3002.
Katrusiak, A. (1995). *Phys. Rev. B*, **51**, 589–592.
Katrusiak, A. (1996*a*). *J. Mol. Struct.* **385**, 71–80.
Katrusiak, A. (1996*b*). *Cryst. Rev.* **5**, 133–180.
Katrusiak, A. (1998). *Pol. J. Chem.* **72**, 449–459.
Katrusiak, A. (2000). *Acta Cryst.* B**56**, 872–881.
Katrusiak, A. (2001). Submitted.
Kitajgorodski, A. I. (1976). *Kryształy molekularne*, pp. 114–121. Warsaw: PWN.
Milstien, S. & Cohen, L. A. (1972). *J. Am. Chem. Soc.* **94**, 9158–9165.
Sheats, J. R. & Barbara, P. F. (1999). (Editors of special issue). *Acc. Chem. Res.* **32**, 191–276.
Sheldrick, G. M. (1986). *SHELXS*86. University of Göttingen, Germany.
Sheldrick, G. M. (1997). *SHELXL*97. University of Göttingen, Germany.
Ziener, V., Breuning, E., Lehn, J.-M., Wegelius, E., Rissanen, K., Baum, G., Fenske, D. & Vannghan, G. (2000). *Chem. Eur. J.* **6**, 4132–4139.

Coupling of the lactone-ring conformation with crystal symmetry in 6-hydroxy-4,4,5,7,8-pentamethyl-3,4-dihydrocoumarin. Erratum

Armand Budzianowski Andrzej Katrusiak,

Faculty of Chemistry, Adam Mickiewicz University, 60-780 Poznań, Grunwaldzka 6, 60-780 Poznan, Poland

In the paper by Budzianowski & Katrusiak (2002) *Acta Cryst.* (2002), B**58**, 125–133 Figs. 5 and 8 on pages 131 and 132 were transposed while adjusting colour details indicated by the authors in the proof. Revised PDF versions of these pages are available in the online version of this erratum, which is available through **Crystallography Journals Online**.

Two fluoradene derivatives: pseudosymmetry, eccentric ellipsoids and a phase transition. Erratum

Aibing Xia, John P. Selegue, Alberto Carrillo, Brian O. Patrick, Sean Parkin and Carolyn Pratt Brock*

Department of Chemistry, University of Kentucky, Lexington, KY 40506-0055, USA

Numerous printing errors in the paper by Xia *et al.* [*Acta Cryst.* (2001), B**57**, 507–516] are corrected.

In the paper by Xia *et al.* (2001) a number of special characters (′, λ, Å, σ, Δ, ö) were omitted in the printed and PDF versions of the article; the HTML version, however, was correct. The corrected version of the paper is now available from **Crystallography Journals Online**.

References

Xia, A., Selegue, J. P., Carrillo, A., Patrick, B. O., Parkin, S. & Brock, C. P. (2001). *Acta Cryst.* B**57**, 507–516.

Group-Theoretical Analysis of Octahedral Tilting in Perovskites. Erratum

Christopher J. Howard[a]* and Harold T. Stokes[b]

[a]Australian Nuclear Science and Technology Organisation, Private Mail Bag 1, Menai NSW 2234, Australia, and [b]Department of Physics and Astronomy, Brigham Young University, Provo, Utah 84602-4675, USA

An error has been noted within Fig. 1 of the paper by Howard & Stokes (1998). There is a group–subgroup relationship between $I4/mcm$ ($a^0a^0c^-$) and $C2/c$ ($a^-b^-b^-$), and this should be indicated on the figure by a continuous line joining the corresponding boxes. The corrected version of the figure is shown here.

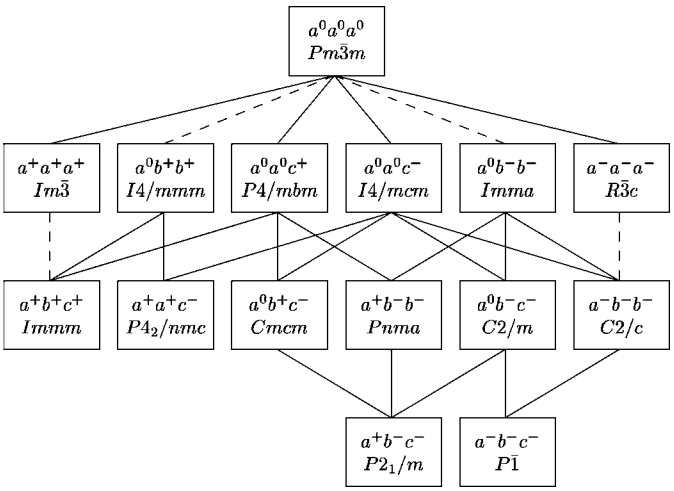

Figure 1
A schematic diagram indicating the group–subgroup relationships among the 15 space groups tabulated by Howard & Stokes (1998). A dashed line joining a group with its subgroup indicates that the corresponding phase transition is required by Landau theory to be first order.

References

Howard, C. J. & Stokes, H. T. (1998). *Acta Cryst.* B**54**, 782–789.